Desalination and Water Treatment
www.deswater.com

doi: 10.5004/dwt.2017.21687

97 (2017) 329–337
November

Equilibrium and kinetics study of reactive dyes removal from aqueous solutions by bentonite nanoparticles

Ali Naghizadeh[a,*], Mohammad Kamranifar[b], Ahmad Reza Yari[c], Mohammad Javad Mohammadi[d]

[a]*Medical Toxicology and Drug abuse Research Center (MTDRC), Birjand University of Medical Sciences (BUMS), Birjand, Iran, Tel. +989126529755; email: aliinaghizadeh@gmail.com*
[b]*Member of Student Research Committee, Department of Environmental Health Engineering, Faculty of Health, Birjand University of Medical Sciences (BUMS), Birjand, Iran, email: kamranifar12@gmail.com*
[c]*Research Center for Environmental Pollutants, Qom University of Medical Sciences, Qom, Iran, email: yari1ahr@gmail.com*
[d]*Abadan School of Medical Sciences, Abadan, Iran, email: javad.sam200@gmail.com*

Received 5 April 2017; Accepted 16 November 2017

ABSTRACT

Today, environmental pollution by various pollutants such as dyes is one of the most important issues of the world. Colored wastewaters are entering to the environment by many industries (for instance, textile and paper industries). Various technologies have been used to remove these pollutants. In this study, we have demonstrated the effectiveness of bentonite nanoparticles as a low cost adsorbent for removal of Reactive Yellow 15 (RY15) and Reactive Yellow 42 (RY42). The effects of variables such as pH, contact time, dye concentrations, adsorbent dosage and solution temperature, on the removal process have been studied. Residual of RY15 and RY42 dyes concentration was measured using a spectrophotometer set in 420 and 430 nm wavelengths, respectively. Also, the bentonite nanoparticles were characterized by scanning electron microscopy, Fourier transform infrared spectroscopy, X-ray diffraction and Brunauer–Emmett–Teller. Finally, the data were examined by isotherms of Langmuir, Freundlich, pseudo-first-order and pseudo-second-order kinetics and thermodynamic parameters. The maximum amount of adsorption for both dyes was at the pH = 3. With increasing the contact time and concentration of dye, adsorption capacity increased as well. Also, increasing the adsorbent dosage resulted decreasing the adsorption capacity. In optimum conditions, the maximum absorption capacity was 156.9 mg/g for RY15 and 170.7 mg/g for RY42. It was shown that removal of dyes of RY15 and RY42 follow, respectively, Freundlich isotherm and Langmuir isotherm and pseudo-second-order kinetics. The results of examining temperature and thermodynamics of the process showed that $\Delta S°$ and $\Delta H°$ are negative for both dyes. However, $\Delta G°$ was positive or negative for different temperatures. Since bentonite nanoparticles of this research were effective, cheap and available, so it can be used as an effective adsorbent for removal of RY15 and RY42.

Keywords: Bentonite nanoparticles; Adsorption; Reactive Yellow dye; Isotherm; Kinetic; Thermodynamic

1. Introduction

Today, environmental pollution is one of the most important global issues [1]. Industrial wastewaters are among the most important pollutants and since these pollutants have different compositions (and elements in their composition), so their treatment is difficult [2]. Among these pollutants, dyes are among the compounds that about one million tons of them are produced in different aspects of modern life [3]. Dye wastewaters are being produced

---

* Corresponding author.

1944-3994/1944-3986

in many industries (such as textile, paper, printing, food industries, health and cosmetic materials) and entered into the environment [4,5].

Textile dyes are the biggest category of synthetic dyes that are solvable in water and their chemical structures have the most diverse structures [6]. Based on chemical structure, dyes are divided to azo, anthraquinone, heterocyclic, phthalocyanine dye and based on their application method, they are divided to reactive, acidic, direct, vat, disperse and etc [7].

Dyes are distinguishable in small quantities and can cause harm on the life of marine life and public health [8]. Studies have shown that textile dyes can cause cancer and genetic mutations also can cause allergy, dermatitis and skin irritation [9,10]. Also, entering of the colored wastewaters to the waters is damaging the aesthetic nature of the environment [11]. Dyes form chemical compounds with metallic ions and therefore can form compounds that are poisonous for fish and other microorganisms that live in water [12].

Various techniques, such as coagulation, chemical oxidation, biological treatment, electrochemical, ion exchange, adsorption, ozonation–coagulation and coagulation–ion exchange have been used for the removal of dye from wastewaters [13,14]. The common methods of wastewater treatment (such as coagulation and chemical sedimentation) are not considered as effective methods for removal of dyes, because most of textile dyes are non-biodegradable and also because these methods produce a lot of sludge [15]. Advanced treatment processes are usually expensive and require expert personnel to be implemented [16]. Biological treatment is not satisfactory, because many of dyes are complex chemical structure and synthetic organic origin. [17].

Among other methods, the adsorption process has a high potential in removing the fine-molecular materials such as heavy metals and dyes, and it seems that this method is one of the best methods for the treatment of wastewaters [18,19]. The adsorption process has many benefits over other conventional methods. These include low sensitivity to currency changes, absence of poisonous materials in the process, high flexibility in the design and operation of the process [20]. Most adsorbents that used for removal of various dyes from wastewater are chitin and chitosan [21], single-wall carbon nanotubes [22], bone char [23], activated carbons from walnut shells [24].

Activated carbon is among the most used adsorbents that is applicable for adsorbing of dyes, but regarding to high cost and difficulty of its regeneration, there are some studies underway to get some adsorbents that have less expenses and higher rates of removal [25].

Elmoubarki et al. [26] studied the effectiveness of clay for removal of textile dyes from water solutions; it was shown that with increasing the adsorbent dosage, contact time and decreasing the pH, removal of dye increased. Also, Tahir and Rauf [27] performed a research and showed that bentonite clay is effective for removal of malachite green (maximum adsorption 90%). In another study by Nourmoradi et al [10], the removal of NB (navy blue CE-RN) dye by combined process of coagulation–flocculation followed by adsorption, it was shown that removal of NB dye has been done well and in acidic pH. Finally, the results of this study showed that C–F followed by adsorption techniques can be considered as an excellent alternative for the treatment of NB containing wastewaters, this removal process was better. In another study by Afkhami and Moosavi [28], the removal of congo red by maghemite nanoparticles, it was showed that the maximum adsorption occurred at pH 5.9. Also, the results of this study show that Langmuir model is almost more successful in representing experimental isotherm data for the adsorption of CR on maghemite nanoparticles. According to the isotherm, maximum adsorption capacity was 208.33 mg/g.

Today nanotechnology methods are being considered more and more. Nanoparticles are very small size, have large surface areas, are crystal shaped and have high reactivity; therefore, these nanomaterials can be used for removal of the pollutants [29]. In recent years, a lot of studies have been done on the usage of clay for removal of various pollutants from environment. Nanoclay is one of the low cost nanomaterials. It has some characteristics like not being poisonous for the environment, high adsorption capacity and high specific surface area [30]. In this study, bentonite nanoparticles were used to remove Reactive Yellow 15 (RY15) and Reactive Yellow 42 (RY42) dyes from aqueous solutions. Parameters such as pH, contact time, dye concentration, adsorbent dosage, temperature and thermodynamics of the process were examined. In addition, isotherm and kinetics of removal were studied.

2. Materials and methods

2.1. Materials

In this study, bentonite nanoparticles were purchased from Pishgaman Nano Materials Company (Iran). The characteristics of bentonite nanoparticles were determined using scanning electron microscopy (SEM), Fourier transform infrared spectroscopy (FTIR), X-ray diffraction (XRD) and Brunauer–Emmett–Teller (BET) analyzes. The dyes that were used in the study (RY15 and RY42) were supplied by Alvansabet Company (Iran). Chemical structures of these dyes have been shown in Figs. 1 and 2, respectively. Maximum wavelength of adsorption for RY15 is 420 nm and for RY42 is 430 nm. Other chemicals used in this study were from Merck (Germany).

2.2. Adsorption experiments

For adsorption stage experiments, a stock solution of dye was prepared (1,000 mg/L) by dissolving required amount of RY15 or RY42 dyes in distilled water. We used UV/VIS spectrophotometer (UV/VIS spectrophotometer T80$^+$, PG Instrument Ltd., British) for measuring the removal of dye.

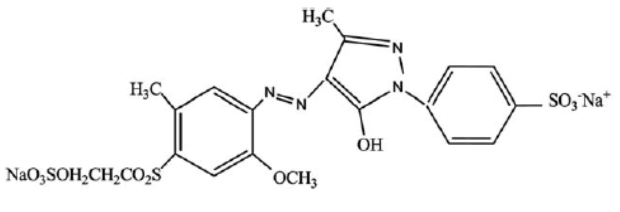

Fig. 1. Chemical structure of Reactive Yellow 15 (RY15) [32].

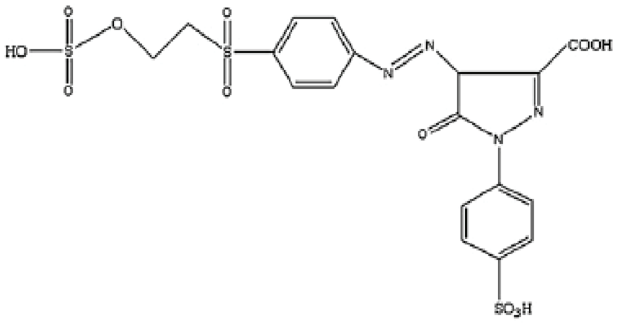

Fig. 2. Chemical structure of Reactive Yellow 42 (RY42) [33].

For adjusting the pH of the solutions, we used HCl and NaOH 1 N (pH meter Knick, 765 cliamatic). These experiments were done in batch system and examined parameters including initial pH (3–11), contact time (2–120 min), initial concentration of dye (20–60 mg/L), solution temperatures (288, 298, 308, and 323 K) were all studied.

2.2.1. *Effect of initial pH*

The effect of pH on dye removal was studied by varying the pH of the dye solution from 3 to 11 (dye concentration 40 mg/L and dosage adsorbent 0.4 g/L). The solutions (100 mL) were put in 250 mL Erlenmeyer flasks and were put on the orbital shaker (Orbital shaker, Mode KS260C) and shaken with the speed of 250 rpm for 60 min. After this time, the concentration of dye was determined by UV–Visible spectrophotometer.

2.2.2. *Effect of contact time and concentration of dye*

After determining the optimal pH of dye, the effect of initial concentration on the removal of dye was examined using various dye concentrations from 20 to 60 mg/L with adsorbent dosage of 0.4 g/L and at times of 2–120 min.

2.2.3. *Effect of dosage adsorbent*

The effect of dosage adsorbent on the adsorption processes was executed from 0.2 to 0.6 g/L with optimal pH, contact time and optimal concentration of dye. After equilibrium, the adsorbent was separated by filtration and the filtrate was analyzed spectrophotometrically.

The adsorption capacity (q_e) was calculated using the following equation:

$$q_e = \frac{C_0 - C_e}{m} V \tag{1}$$

where q_e (mg/L) is the capacity of adsorption of dye, C_0 (mg/L) is the initial concentration of dye, C_e (mg/L) is the concentration of remaining dye, m (g) is adsorbent dosage and V (L) is the sample volume [33].

2.3. *Temperature and thermodynamics of adsorption process*

The effect of temperature and thermodynamics of the adsorption process with keeping constant of optimal parameters (pH, contact time, adsorbent dosage and dye concentration) at different temperatures of 288, 298, 308 and 323 K were studied. For this stage, the shaker incubator (COMBI-SHAKER, Model NB-101MT) was used. Different thermodynamic constants of adsorption such as Gibb's free energy ($\Delta G°$), entropy ($\Delta S°$) and enthalpy ($\Delta H°$) were determined using Eqs. (2), (3) and (4).

$$k_d = \frac{q_e}{C_e} \tag{2}$$

$$\Delta G° = -RT \ln k_d \tag{3}$$

$$\ln k_d = -\frac{\Delta H°}{RT} + \frac{\Delta S°}{R} \tag{4}$$

In above equations, R is the universal constant of the gases (8.314 J/mol K), T is the absolute temperature and k_d is the thermodynamics equilibrium [5].

2.4. *Adsorption isotherms*

Isotherms were obtained by measuring the dye concentration at equilibrium (dye concentrations 20–60 mg/L). The Langmuir and Freundlich models were used to fit the experimental equilibrium adsorption data. The equations of these models are as follows [34]:

$$q_e = K_f C_e^{\frac{1}{n}} \tag{5}$$

where q_e (mg/g) is the amount of adsorbed dye in adsorbent, C_e (mg/L) is the concentration of remaining dye in the solution at equilibrium time and K_f are constants of Freundlich equation.

$$q_e = \frac{Q_m K_L C_e}{1 + K_L C_e} \tag{6}$$

where Q_m is the maximum amount of adsorbed dye in adsorbent (mg/g), K_L is the constant of Langmuir equation [35].

2.5. *Kinetics of adsorption*

The kinetics of adsorption (pseudo-first-order and pseudo-second-order of kinetics) was determined at five different dye concentrations from 20 to 60 mg/L. The kinetics equations are as follows:

$$\frac{dq_t}{dt} = K_1 (q_e - q_t) \tag{7}$$

$$\frac{dq_t}{dt} = K_2 (q_e - q_t)^2 \tag{8}$$

In these equations, q_e (mg/g) is the amount of adsorbed dye at equilibrium time, q_t (mg/g) is the amount of adsorbed dye at time, K_1 (1/min) is the constant of pseudo-first-order kinetics and K_2 (g/mg min) is the constant of pseudo-second-order kinetics [36].

3. Results and discussion

3.1. Characteristics of adsorbent

SEM is a main and powerful magnification tool for study of the morphological structure of adsorbents [37]. Fig. 3 shows SEM images of bentonite nanoparticles. The images show that bentonite nanoparticles have layer structure. The thickness of this layer is estimated between 29 and 62 nm.

The results of the BET analysis showed that the surface area of bentonite nanoparticles is 46.58 m^2/g (Fig. 4).

According to Fig. 5, the band of 3,435.61 cm^{-1} assigned as amine N–H stretching. Primary amines produce two N–H stretching adsorptions, secondary amides only one, and tertiary none. The band of 1,637.30 cm^{-1} is related to alkenyl C=C stretching. The band of 1,035.32 cm^{-1} is related to Si–O stretching, clay minerals. Furthermore the bands at the range of 680–860 cm^{-1} can be assigned as aromatic C–H bending. Also the band at 530.46 cm^{-1} belongs to Fe–O, Fe_2O_3 and Si–O–Al stretching. The bands at 468.61 cm^{-1} can be assigned to Si–O–Si bending. FTIR analysis characterizes materials, and is especially useful in recognizing inorganic mixtures. FTIR, as Raman spectroscopy, can provide the molecular and structural information about organic and inorganic materials.

XRD patterns of the bentonite nanoparticles show a medium peak at $2\theta = 6.05°$ and also a sharp peak at $2\theta = 27.80°$ that corresponds to the nanostructures of the adsorbents (Fig. 6).

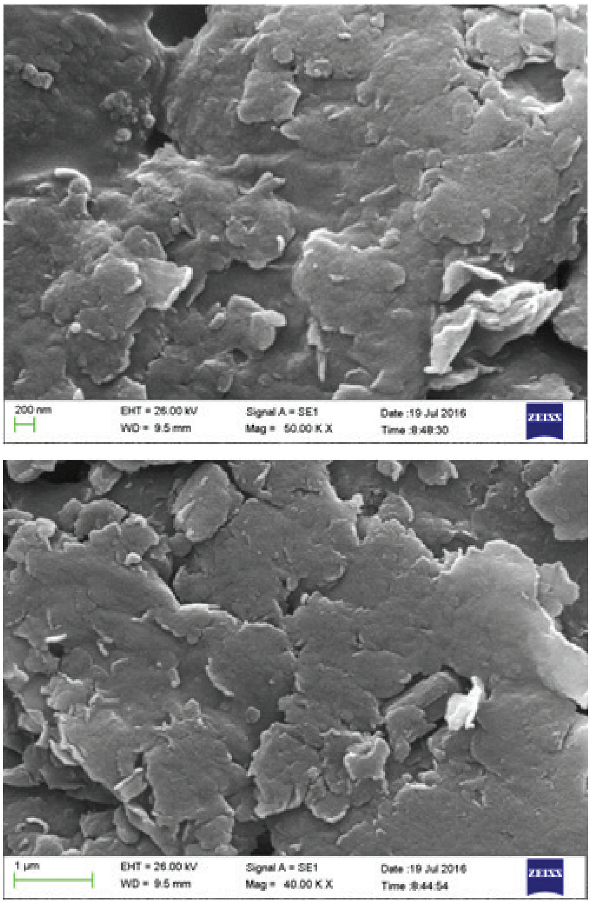

Fig. 3. SEM images of the bentonite nanoparticles.

3.2. Effects of pH on the removal of dye

Amount of pH of solution is one of the important parameters that affect the adsorption capacity of the adsorbents [38,39]. pH of the solution is very important in the adsorption process of dyes, because it affects the chemical sites of adsorbent surface area and also it affects the surface charge of the adsorbent, molecular structure of dye and ionization degree of different pollutants [40]. In order to examine the effects of pH on the adsorption of dye by the bentonite nanoparticles, we prepared solutions with the concentration of 40 mg/L,

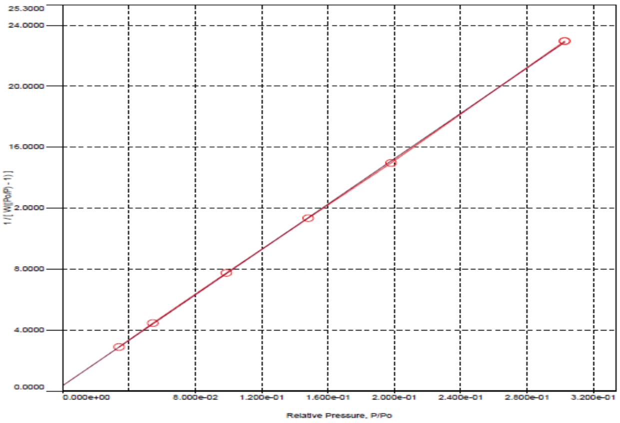

Fig. 4. BET analysis of the bentonite nanoparticles.

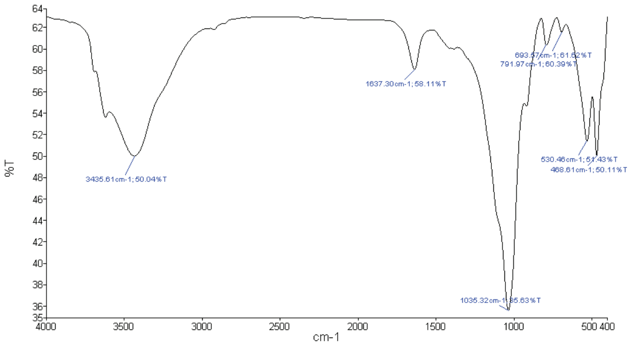

Fig. 5. FTIR spectra of the bentonite nanoparticles.

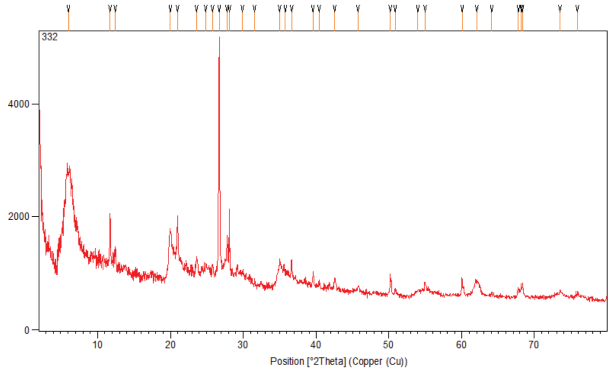

Fig. 6. XRD pattern of the bentonite nanoparticles.

pH (3–11) and adsorbent dosage of 0.4 g/L for 60 min, and the results can be seen in Figs. 7 and 8. According to the results, with increasing the pH, adsorption decreased. As it can be seen in these results, the maximum amount of adsorption for both dyes (RY15 and RY42) was at the pH = 3, when the adsorption capacity was 66.3 mg/g for RY15 and 81.2 mg/g for RY42. At higher pH, because OH^- is abundant, the possibility of repellent force between the adsorbent and dye is high, because both of them have negative charges [41]. On this issue, Asgher and Bhatti [42] have reached to the similar results.

3.3. Effects of contact time and concentration on the removal of dye

In this study, effects of contact time were studied by changing time from 2 to 120 min, pH = 3, initial amount of adsorbent 0.4 g/L, dye concentrations (20–60 mg/L). As it can be seen in Figs. 9 and 10, as contact time and concentration of dye increased, adsorption capacity increased as well and the maximum amount of adsorption occurred at the first moments. According to the results, maximum amount of adsorption for these dyes occurred at the concentration of 60 mg/L and time of 15 min and after this time the adsorption does not increase much and reaches to the equilibrium. This object is because of many empty holes on the adsorbent surface and after those holes is filled by dye molecules, and then the repellent force between the adsorbent and dyes increases and adsorption decreases [43]. These results agree with the studies of Bhattacharyya and Ray [5] and Cengiz and Cavas [44]. Also, the results of effects of concentration of dye on the rate of adsorption show that with increasing the concentration of dye, the adsorption capacity for both dyes increases (Figs. 9 and 10), as when time = 15 min and pH = 3, then increasing the concentration of dye from 20 to 60 mg/L increases the adsorption level for RY15 from 40.8 to 89.8 mg/g and this amount increases from 40.2 to 119.4 mg/g for RY42. This can happen because with increasing the concentration of dyestuff molecules, the contact between the dyestuff molecules and adsorbent molecules increases and this can increase the adsorption of dye by adsorbent. And this finally increases the adsorption capacity [45]. The results of a study by Khattri and Singh [46] confirm the results of this study.

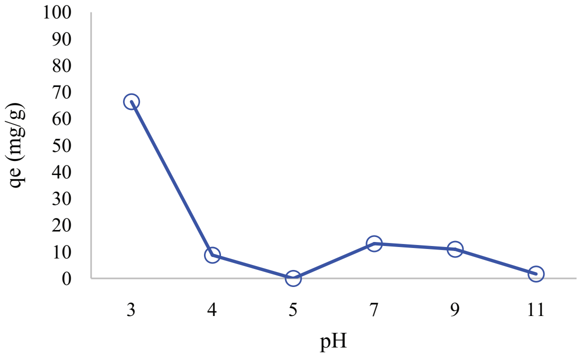

Fig. 7. Effects of pH on the removal of dye (RY15) by bentonite nanoparticles.

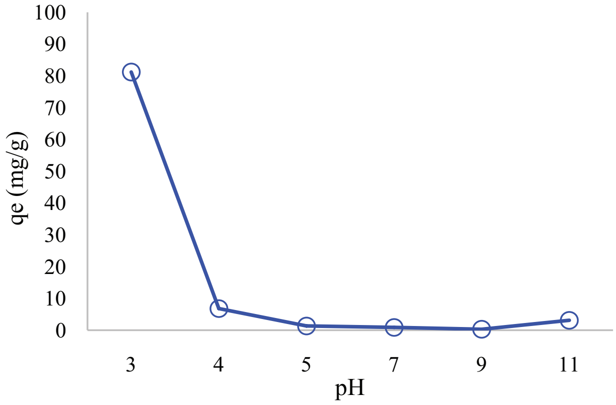

Fig. 8. Effects of pH on the removal of dye (RY42) by bentonite nanoparticles.

3.4. Effects of adsorbent dosage on the removal of dye

Adsorbent dosage is an important parameter in adsorption process, because it determines the capacity of adsorbent for a concentration of pollutant [47]. At this study, the effects of adsorbent dosage were studied on the adsorption of dye at pH = 3, contact time = 15 min, dye concentration 60 mg/L and we examined five different dosages (0.2–0.6 g/L).

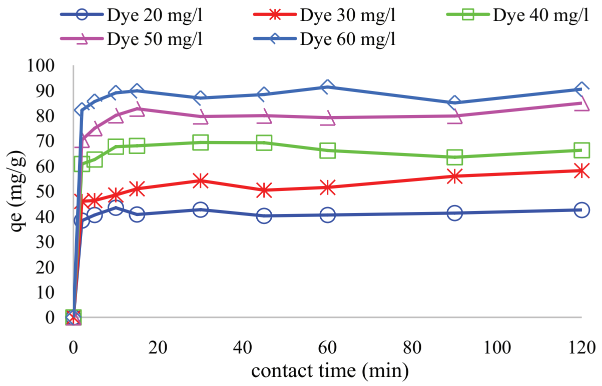

Fig. 9. Effects of contact time and dye concentration on the removal of RY15 by bentonite nanoparticles.

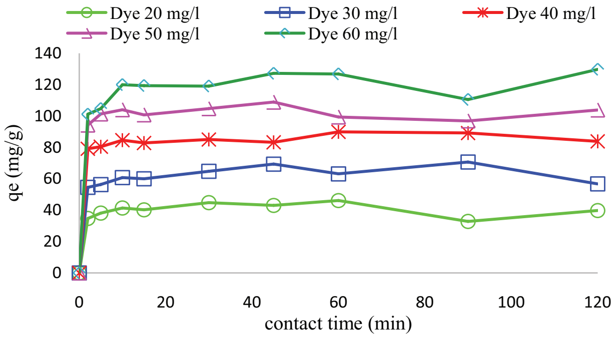

Fig. 10. Effects of contact time and dye concentration on the removal of RY42 by bentonite nanoparticles.

Figs. 11 and 12 have shown the effects of adsorbent dosage on the removal of RY15 and RY42. As it can be seen from Fig. 11, with increasing the adsorbent dosage of 0.2–0.6 g/L, the adsorption capacity decreased from 157 to 61 mg/g. And with increasing the adsorbent dosage for RY42, the adsorption capacity decreased from 170 to 82 mg/g (Fig. 12). For interpreting this result, it can be said that with increasing the amount of adsorbent in similar situation, the active sites for the interactions between the adsorbent and pollutant increases [48] and along these lines, adsorption capacity by bentonite nanoparticles decreases and this can be because of not using the entire capacity of the adsorbent and with increasing the adsorbent, some active places of the adsorbent remain unsaturated and so the adsorption of the pollutant decreases [49]. Jarusiripot [50] reached to the similar results.

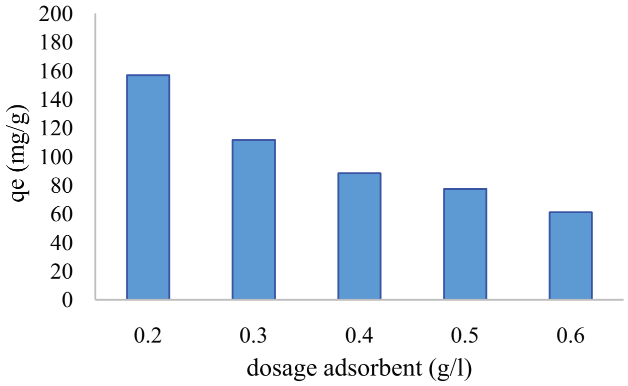

Fig. 11. Effects of increasing the adsorbent dosage on the removal of RY15 by bentonite nanoparticles.

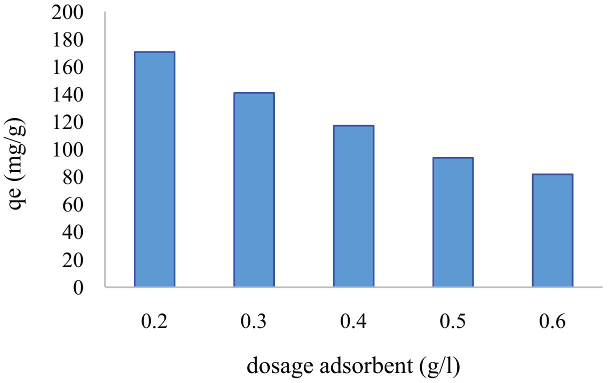

Fig. 12. Effects of increasing the adsorbent dosage on the removal of RY42 by bentonite nanoparticles.

3.5. Effects of temperature and thermodynamics

At this stage, the effects of temperature on the removal dye by bentonite nanoparticles were studied. For this matter, the dyed solution with concentration = 60 mg/L, pH = 3, dosage adsorbent = 0.2 g/L, contact time = 15 min, was in temperatures of 288, 298, 308 and 323 K and the results are shown in Table 1.

The results of the thermodynamics studies are shown in Table 1. For RY15 dye, the negative amount of $\Delta H°$ for all temperatures shows that adsorption of RY15 by bentonite nanoparticles is an exothermic process. Also, the negative amount of $\Delta G°$ shows that dye adsorption by bentonite nanoparticles is a spontaneous reaction and positive amount of this parameter shows that the process is possible but non-spontaneous. The value of $\Delta S°$ is negative which means that the dye molecules at the solid–liquid interface are more organized than those in the bulk solution phase [52].

3.6. Isotherm of adsorption

Isotherms are significant for describing the partitioning of pollutants in environmental systems [53]. The results of Langmuir and Freundlich models for RY15 and RY42 were studied and are shown in Table 2. As shown in Table 2, adsorption of RY15 dye by bentonite nanoparticles with $R^2 = 1$ follows the Freundlich isotherm ($R^2 = 1$) to a great extent and this shows that the surface of bentonite nanoparticles is heterogenous and the adsorption of RY15 dye was layer by layer. Observations other researchers confirm the results of this study [54]. However, adsorption of RY42 dye by bentonite nanoparticles followed the Langmuir isotherm ($R^2 = 0.94$) and according to this model, the dye adsorption was single layer and homogenous. Langmuir model estimated the maximum amount of dye adsorption around 315 mg/g and this number is close to the equilibrium capacity of this research. Inclination of adsorption of RY42 dye by adsorbent was examined by a non-dimensional parameter (R_L) that was derived from Langmuir model. If $R_L = 0$ then the adsorption is irrevocable and if $R_L = 1$ the adsorption is linear, if $1 < R_L$ then the adsorption is unfavorable and if $0 < R_L < 1$ then the adsorption is favorable. According to the results of Langmuir isotherm for RY42, R_L is between 0 and 1, so the adsorption process by bentonite nanoparticles is favorable [55].

Table 1
Thermodynamic parameters of adsorption of RY15 and RY42 by bentonite nanoparticles

T (K)	RY15				RY42			
	$\Delta G°$ (kJ/mol)	$\Delta H°$ (kJ/mol)	$\Delta S°$ (J/mol K)	R^2	$\Delta G°$ (kJ/mol)	$\Delta H°$ (kJ/mol)	$\Delta S°$ (J/mol K)	R^2
288	–0.60	–18,851.5	–62.15	0.75	–0.63	–39,171.7	–131.55	0.79
298	–0.48				–0.22			
308	–0.39				0.06			
323	1.70				4.22			

3.7. Kinetics of adsorption

Also in this study, pseudo-first-order and pseudo-second-order kinetics were studied. According to Table 3, by comparing the amounts of R^2 for RY15 and RY42, it is clear that the adsorption of dye for these dyes follows the pseudo-second-order kinetics. On the other hand, with studying the pseudo-second-order equations, it can be seen that there is little difference between capacity of adsorption under empirical equilibrium conditions (q_{cal}) and the capacity of adsorption under calculation based conditions (q_{exp}). Hence, pseudo-second-order kinetic model can be used properly for explaining the kinetics of these dyes with bentonite nanoparticles. The findings of Gök et al. [56] confirm these findings.

Table 2
The results of isotherm calculations for RY15 and RY42 adsorption onto bentonite nanoparticles

Isotherm	Constants	Values	
		RY15	RY42
Freundlich	R^2	1.00	0.93
	K_f (mg/g)	16.81	9.71
	n	1.95	1.07
	$1/n$	0.51	0.93
Langmuir	R^2	0.98	0.94
	R_L	0.13	0.37
	K_L (L/mg)	0.085	0.012
	q_{max} (mg/g)	124.06	787.59

3.8. Comparison of the adsorbent with other adsorbents

Table 4 compares the maximum absorption capacity of this adsorbent with other adsorbents used to remove various dyes.

4. Conclusions

This study showed that bentonite nanoparticles can be an effective adsorbent for removal of RY15 and RY42 dyes. In the optimal conditions of the experiment (pH = 3, contact time = 15 min, dye concentration = 60 mg/L, adsorbent dosage = 0.2 g/L), the adsorption capacity for RY15 = 156.9 mg/L and RY42 = 170.7 mg/L. Finally, since bentonite nanoparticles are low cost and available, so it can be used as an effective adsorbent for removal of RY15 and RY42 dyes.

Table 3
Kinetic constants calculations for adsorption of RY15 and RY42 onto bentonite nanoparticles

Dye	C_0 (mg/L)	Pseudo-first-order			Pseudo-second-order			$q_{e,\mathrm{exp}}$ (mg/g)
		K_1 (min^{-1})	$q_{e,\mathrm{cal}}$ (mg/g)	R^2	K_2 (g/mg min)	$q_{e,\mathrm{cal}}$ (mg/g)	R^2	
RY15	22	0.00	2.55	0.00	0.06	42.04	1.00	44.47
	29	0.01	8.18	0.25	0.01	57.32	0.99	59.19
	41	0.00	2.61	0.03	0.04	65.39	1.00	70.36
	54	0.01	6.24	0.12	0.01	83.09	1.00	85.96
	64	0.00	3.75	0.02	0.07	88.95	1.00	92.37
RY42	20	0.00	4.05	0.02	0.02	37.77	0.95	47.15
	32	0.00	6.90	0.02	0.01	61.05	0.97	71.70
	42	0.00	5.40	0.04	0.35	86.02	0.99	90.94
	52	0.00	4.89	0.02	0.07	101.42	0.99	109.88
	63	0.01	12.47	0.16	0.01	124.14	0.99	130.73

Table 4
Comparison of the maximum adsorption capacity ($q_{e,\mathrm{max}}$) of bentonite nanoparticles for removal of RY15 and RY42 dyes with other adsorbents used to removal of Reactive Yellow dye

Adsorbent	Adsorbate	q_m (mg/g)	Reference
Bentonite nanoparticles	Reactive Yellow 15	156.9	This study
Bentonite nanoparticles	Reactive Yellow 42	170.7	This study
Setaria verticillata carbon	Reactive Yellow 15	138.6	[32]
Citrus sinensis biomass (free)	Reactive Yellow 42	36.3	[42]
Citrus sinensis biomass (immobilized)	Reactive Yellow 42	51.4	[42]
Citrus sinensis biomass (acetic acid treated)	Reactive Yellow 42	106.3	[42]
Magnetite nanoparticles	Reactive Yellow 145	76.9	[57]
Hydroxypatite	Reactive Yellow 84	50.2	[58]
Calcined alunite	Reactive Yellow 64	236	[59]
Fly ash	Reactive Yellow HED	37.2	[60]

References

[1] M.J. Mohammadi, A. Takdastan, S. Jorfi, A. Neisi, M. Farhadi, A.R. Yari, S. Dobaradaran, Y.O. Khaniabadi, Electrocoagulation process to chemical and biological oxygen demand treatment from carwash grey water in Ahvaz megacity, Iran, Data in Brief, 11 (2017) 634–639.

[2] V.K. Garg, R. Gupta, A. Bala Yadav, R. Kumar, Dye removal from aqueous solution by adsorption on treated sawdust, Bioresour. Technol., 89 (2003) 121–124.

[3] G. Hassani, A. Babaei, A. Takdastan, M. Shirmardi, F. Yousefian, M. Mohammadi, Occurrence and fate of 17β-estradiol in water resources and wastewater in Ahvaz, Iran, Global Nest J., 18 (2016) 855–866.

[4] K. Vijayaraghavan, Y.-S. Yun, Biosorption of C.I. Reactive Black 5 from aqueous solution using acid-treated biomass of brown seaweed *Laminaria* sp, Dyes Pigm., 76 (2008) 726–732.

[5] R. Bhattacharyya, S.K. Ray, Removal of congo red and methyl violet from water using nano clay filled composite hydrogels of poly acrylic acid and polyethylene glycol, Chem. Eng. J., 260 (2015) 269–283.

[6] N. Azbar, T. Yonar, K. Kestioglu, Comparison of various advanced oxidation processes and chemical treatment methods for COD and color removal from a polyester and acetate fiber dyeing effluent, Chemosphere, 55 (2004) 35–43.

[7] X.-R. Xu, H.-B. Li, W.-H. Wang, J.-D. Gu, Degradation of dyes in aqueous solutions by the Fenton process, Chemosphere, 57 (2004) 595–600.

[8] Z. Aksu, S. Ertuğrul, G. Dönmez, Methylene Blue biosorption by *Rhizopus arrhizus*: effect of SDS (sodium dodecylsulfate) surfactant on biosorption properties, Chem. Eng. J., 158 (2010) 474–481.

[9] B. Royer, N.F. Cardoso, E.C. Lima, J.C.P. Vaghetti, N.M. Simon, T. Calvete, R.C. Veses, Applications of Brazilian pine-fruit shell in natural and carbonized forms as adsorbents to removal of methylene blue from aqueous solutions—kinetic and equilibrium study, J. Hazard. Mater., 164 (2009) 1213–1222.

[10] H. Nourmoradi, S. Zabihollahi, H. Pourzamani, Removal of a common textile dye, navy blue (NB), from aqueous solutions by combined process of coagulation–flocculation followed by adsorption, Desal. Wat. Treat., 57 (2015) 1–12.

[11] A.R. Dinçer, Y. Güneş, N. Karakaya, E. Güneş, Comparison of activated carbon and bottom ash for removal of reactive dye from aqueous solution, Bioresour. Technol., 98 (2007) 834–839.

[12] R. Malik, D.S. Ramteke, S.R. Wate, Adsorption of malachite green on groundnut shell waste based powdered activated carbon, Waste Manage., 27 (2007) 1129–1138.

[13] S. Abo-Farha, Comparative study of oxidation of some azo dyes by different advanced oxidation processes: Fenton, Fenton-like, photo-Fenton and photo-Fenton-like, J. Am. Sci., 6 (2010) 128–142.

[14] Z. Eren, F.N. Acar, Adsorption of Reactive Black 5 from an aqueous solution: equilibrium and kinetic studies, Desalination, 194 (2006) 1–10.

[15] K.-s. Wang, H.-Y. Chen, L.-C. Huang, Y.-C. Su, S.-H. Chang, Degradation of Reactive Black 5 using combined electrochemical degradation-solar-light/immobilized TiO_2 film process and toxicity evaluation, Chemosphere, 72 (2008) 299–305.

[16] A.R. Rahmani, G. Asgari, M. Farrokhi, Removal of Reactive Black 5 (RB5) dye from aqueous solution using adsorption onto strongly basic anion exchange resin: equilibrium and kinetic study, Iran. J. Health Environ., 5 (2013) 509–518.

[17] G. Crini, Non-conventional low-cost adsorbents for dye removal: a review, Bioresour. Technol., 97 (2006) 1061–1085.

[18] A. Naghizadeh, Comparison between activated carbon and multiwall carbon nanotubes in the removal of cadmium(II) and chromium(VI) from water solutions, J. Water Supply Res. Technol. AQUA, 64 (2015) 64–73.

[19] A. Naghizadeh, M. Ghafouri, A. Jafari, Investigation of equilibrium, kinetics and thermodynamics of extracted chitin from shrimp shell in reactive blue 29 (RB-29) removal from aqueous solutions, Desal. Wat. Treat., 70 (2017) 355–363.

[20] N.P. Bhagya, P.A. Prashanth, R.S. Raveendra, S. Sathyanarayani, S. Ananda, B.M. Nagabhushana, H. Nagabhushana, Adsorption of hazardous cationic dye onto the combustion derived $SrTiO_3$ nanoparticles: kinetic and isotherm studies, J. Asian Ceram. Soc., 4 (2016) 68–74.

[21] S. Ling, C. Yee, H. Eng, Removal of a cationic dye using deacetylated chitin/chitosan, J. Appl. Sci., 11 (2011) 1445–1448.

[22] I.M. Jauris, S.B. Fagan, M.A. Adebayo, F.M. Machado, Adsorption of acridine orange and methylene blue synthetic dyes and anthracene on single wall carbon nanotubes: a first principle approach, Comput. Theor. Chem., 1076 (2016) 42–50.

[23] A.W.M. Ip, J.P. Barford, G. McKay, A comparative study on the kinetics and mechanisms of removal of Reactive Black 5 by adsorption onto activated carbons and bone char, Chem. Eng. J., 157 (2010) 434–442.

[24] J. Yang, K. Qiu, Preparation of activated carbons from walnut shells via vacuum chemical activation and their application for methylene blue removal, Chem. Eng. J., 165 (2010) 209–217.

[25] W. Balla, A.H. Essadki, B. Gourich, A. Dassaa, H. Chenik, M. Azzi, Electrocoagulation/electroflotation of reactive, disperse and mixture dyes in an external-loop airlift reactor, J. Hazard. Mater., 184 (2010) 710–716.

[26] R. Elmoubarki, F. Mahjoubi, H. Tounsadi, J. Moustadraf, M. Abdennouri, A. Zouhri, A. El Albani, N. Barka, Adsorption of textile dyes on raw and decanted Moroccan clays: kinetics, equilibrium and thermodynamics, Water Resour. Ind., 9 (2015) 16–29.

[27] S. Tahir, N. Rauf, Removal of a cationic dye from aqueous solutions by adsorption onto bentonite clay, Chemosphere, 63 (2006) 1842–1848.

[28] A. Afkhami, R. Moosavi, Adsorptive removal of Congo red, a carcinogenic textile dye, from aqueous solutions by maghemite nanoparticles, J. Hazard. Mater., 174 (2010) 398–403.

[29] A. Dalvand, R. Nabizadeh, M. Reza Ganjali, M. Khoobi, S. Nazmara, A. Hossein Mahvi, Modeling of Reactive Blue 19 azo dye removal from colored textile wastewater using L-arginine-functionalized Fe_3O_4 nanoparticles: optimization, reusability, kinetic and equilibrium studies, J. Magn. Magn. Mater., 404 (2016) 179–189.

[30] D.W. Litchfield, D.G. Baird, The role of nanoclay in the generation of poly(ethylene terephthalate) fibers with improved modulus and tenacity, Polymer, 49 (2008) 5027–5036.

[31] T. Vidhyadevi, A. Murugesan, S. Kalaivani, M. Anil Kumar, K. Thiruvenkada Ravi, L. Ravikumar, C. Anuradha, S. Sivanesan, Optimization of the process parameters for the removal of reactive yellow dye by the low cost *Setaria verticillata* carbon using response surface methodology: thermodynamic, kinetic, and equilibrium studies, Environ. Prog. Sustain. Energy, 33 (2014) 855–865.

[32] M. Asgher, H.N. Bhatti, Evaluation of thermodynamics and effect of chemical treatments on sorption potential of *Citrus* waste biomass for removal of anionic dyes from aqueous solutions, Ecol. Eng., 38 (2012) 79–85.

[33] A. Naghizadeh, H. Shahabi, F. Ghasemi, A. Zarei, Synthesis of walnut shell modified with titanium dioxide and zinc oxide nanoparticles for efficient removal of humic acid from aqueous solutions, J. Water Health, 14 (2016) 989–997.

[34] R. Varadarajan, G. Venkatesan, G. Swaminathan, Removal of copper using clay admixed with quarry fines as landfill liners, Pol. J. Environ. Stud., 25 (2016) 377–384.

[35] A. Naghizadeh, R. Nabizadeh, Removal of reactive blue 29 dye by adsorption on modified chitosan in the presence of hydrogen peroxide, Environ. Prot. Eng., 42 (2016) 149–168.

[36] A. Naghizadeh, K. Gholami, Bentonite and montmorillonite nanoparticles effectiveness in removal of fluoride from water solutions, J. Water Health, 15 (2017) 555–565.

[37] M.E. Mahmoud, G.M. Nabil, N.M. El-Mallah, H.I. Bassiouny, S. Kumar, T.M. Abdel-Fattah, Kinetics, isotherm, and thermodynamic studies of the adsorption of reactive red 195 A dye from water by modified switchgrass biochar adsorbent, J. Ind. Eng. Chem., 37 (2016) 156–167.

[38] Y. Li, F. Liu, B. Xia, Q. Du, P. Zhang, D. Wang, Z. Wang, Y. Xia, Removal of copper from aqueous solution by carbon nanotube/calcium alginate composites, J. Hazard. Mater., 177 (2010) 876–880.

[39] A. Afkhami, M. Saber-Tehrani, H. Bagheri, Modified maghemite nanoparticles as an efficient adsorbent for removing some cationic dyes from aqueous solution, Desalination, 263 (2010) 240–248.

[40] L. Ai, C. Zhang, F. Liao, Y. Wang, M. Li, L. Meng, J. Jiang, Removal of methylene blue from aqueous solution with magnetite loaded multi-wall carbon nanotube: kinetic, isotherm and mechanism analysis, J. Hazard. Mater., 198 (2011) 282–290.

[41] A. Özcan, Ç. Ömeroğlu, Y. Erdoğan, A.S. Özcan, Modification of bentonite with a cationic surfactant: an adsorption study of textile dye Reactive Blue 19, J. Hazard. Mater., 140 (2007) 173–179.

[42] M. Asgher, H.N. Bhatti, Mechanistic and kinetic evaluation of biosorption of reactive azo dyes by free, immobilized and chemically treated *Citrus sinensis* waste biomass, Ecol. Eng., 36 (2010) 1660–1665.

[43] P. Luo, Y. Zhao, B. Zhang, J. Liu, Y. Yang, J. Liu, Study on the adsorption of Neutral Red from aqueous solution onto halloysite nanotubes, Water Res., 44 (2010) 1489–1497.

[44] S. Cengiz, L. Cavas, Removal of methylene blue by invasive marine seaweed: *Caulerpa racemosa* var. *cylindracea*, Bioresour. Technol., 99 (2008) 2357–2363.

[45] M.A. Al-Ghouti, M.A.M. Khraisheh, M.N.M. Ahmad, S. Allen, Adsorption behaviour of methylene blue onto Jordanian diatomite: a kinetic study, J. Hazard. Mater., 165 (2009) 589–598.

[46] S.D. Khattri, M.K. Singh, Removal of malachite green from dye wastewater using neem sawdust by adsorption, J. Hazard. Mater., 167 (2009) 1089–1094.

[47] M.H. Ehrampoush, G. Ghanizadeh, M.T. Ghaneian, Equilibrium and kinetics study of reactive red 123 dye removal from aqueous solution by adsorption on eggshell, Iran. J. Environ. Health Sci. Eng., 8 (2011) 101–108.

[48] V. Vimonses, B. Jin, C.W.K. Chow, C. Saint, Enhancing removal efficiency of anionic dye by combination and calcination of clay materials and calcium hydroxide, J. Hazard. Mater., 171 (2009) 941–947.

[49] K.V. Kumar, K. Porkodi, Mass transfer, kinetics and equilibrium studies for the biosorption of methylene blue using *Paspalum notatum*, J. Hazard. Mater., 146 (2007) 214–226.

[50] C. Jarusiripot, Removal of Reactive Dye by adsorption over chemical pretreatment coal based bottom ash, Procedia Chem., 9 (2014) 121–130.

[51] S. Gueu, B. Yao, K. Adouby, G. Ado, Kinetics and thermodynamics study of lead adsorption on to activated carbons from coconut and seed hull of the palm tree, Int. J. Environ. Sci. Technol., 4 (2007) 11–17.

[52] E. Errais, J. Duplay, F. Darragi, I. M'Rabet, A. Aubert, F. Huber, G. Morvan, Efficient anionic dye adsorption on natural untreated clay: kinetic study and thermodynamic parameters, Desalination, 275 (2011) 74–81.

[53] B. Bina, H. Pourzamani, A. Rashidi, M.M. Amin, Ethylbenzene removal by carbon nanotubes from aqueous solution, J. Environ. Public Health, 2012 (2012) 1–8.

[54] V. Vimonses, S. Lei, B. Jin, C.W.K. Chow, C. Saint, Kinetic study and equilibrium isotherm analysis of Congo Red adsorption by clay materials, Chem. Eng. J., 148 (2009) 354–364.

[55] H. Chen, J. Zhao, J. Wu, G. Dai, Isotherm, thermodynamic, kinetics and adsorption mechanism studies of methyl orange by surfactant modified silkworm exuviae, J. Hazard. Mater., 192 (2011) 246–254.

[56] Ö. Gök, A.S. Özcan, A. Özcan, Adsorption behavior of a textile dye of Reactive Blue 19 from aqueous solutions onto modified bentonite, Appl. Surf. Sci., 256 (2010) 5439–5443.

[57] N.A. Kalkan, S. Aksoy, E.A. Aksoy, N. Hasirci, Adsorption of reactive yellow 145 onto chitosan coated magnetite nanoparticles, J. Appl. Polym. Sci., 124 (2012) 576–584.

[58] N. Barka, S. Qourzal, A. Assabbane, A. Nounah, Y. Ait-Ichou, Removal of Reactive Yellow 84 from aqueous solutions by adsorption onto hydroxyapatite, J. Saudi Chem. Soc., 15 (2011) 263–267.

[59] M. Özacar, İ.A. Şengil, Adsorption of reactive dyes on calcined alunite from aqueous solutions, J. Hazard. Mater., 98 (2003) 211–224.

[60] N. Dizge, C. Aydiner, E. Demirbas, M. Kobya, S. Kara, Adsorption of reactive dyes from aqueous solutions by fly ash: kinetic and equilibrium studies, J. Hazard. Mater., 150 (2008) 737–746.